

Received December 27, 2018, accepted January 4, 2019, date of publication January 10, 2019, date of current version January 29, 2019.

Digital Object Identifier 10.1109/ACCESS.2019.2891763

A Chattering-Free, Adaptive, Robust Tracking Control Scheme for Nonlinear Systems With Uncertain Dynamics

ANH TUAN VO^{ID} AND HEE-JUN KANG^{ID}

School of Electrical Engineering, University of Ulsan, Ulsan 44610, South Korea

Corresponding author: Hee-Jun Kang (hjkang@ulsan.ac.kr)

This research was supported by Basic Science Research Program through the National Research Foundation of Korea (NRF) funded by the Ministry of Education (NRF-2016R1D1A3B03930496).

ABSTRACT This paper introduces a chattering-free, adaptive, and robust tracking control scheme for a class of second-order nonlinear systems with uncertain dynamics. First, a proportional-integral-derivative control-fast terminal sliding function is proposed to enable the advantages of both the PID and non-singular fast terminal sliding mode approaches in the field of non-singularity, fast convergence time, defined time convergence, and stability with small steady-state errors. Second, to obtain the desired control target without chattering behavior, the proposed controller with a continuous approach has been applied. In detail, the proposed controller uses an integral of a switching term and an adaptive updating law to compensate the lumped system uncertainty (e.g., disturbances, unmodeled dynamics, nonlinearities, or unmeasurable noise). Our proposed controller does not require knowledge about bound values of those anonymous components. The robust behavior and the defined time convergence have been demonstrated rigorously by the Lyapunov principle. Finally, the position tracking computer simulations have been performed to demonstrate the effectiveness and practicality of the suggested controller.

INDEX TERMS Proportional-integral-derivative control, non-singular fast terminal sliding mode control, adaptive updating law, finite-time control.

I. INTRODUCTION

The faster the development of modern production systems is, the greater the requirements are for speed, accuracy, reliability, and safety. Further, the more complex a technology is, the more it needs to adopt more advanced technical systems, especially in mechanical structures, sensor systems, and electronic systems. If uncertainty parameters of a system are not accurately calculated and thoroughly resolved, they can reduce the system performance. Moreover, a significant drawback worthy of concern is the delay of the mechanical system generated by friction. To deal with all of the above constraints is a difficult challenge, requiring researchers to propose solutions for performance enhancement. In detail, a robust controller with the ability to counteract or compensate for undesirable terms disturbing the system needs to be developed. Once developed, the system's performance, reliability, and safety will be enhanced.

As reported in the literature, several control algorithms have been successfully adopted to control uncertain nonlinear

systems. Noteworthy examples such as proportional-derivative (PD) or proportional-integral-derivative (PID) controllers [1], [2], intelligent controllers [3]–[8], adaptive controllers [9], [10], synchronization controllers [11], [12], and sliding mode controllers (SMCs) [13]–[22] have been cited. Among these control approaches, SMCs have the best properties to control strongly against perturbations and system uncertainties. However, the classical SMC still has several weaknesses (e.g., significant chattering behavior due to the way to eliminate the chattering in SMC is still missing, undefined time convergence, and ineffective adaptation with rapid variations of perturbations or faults). To treat those obstacles, several recently improved controllers have been suggested and adopted using a nonlinear sliding function in place of a linear sliding function. Those control methodologies are called terminal sliding mode control (TSMC) [23]–[27].

Technically, TSMC carries a defined time convergence but attaches a singularity matter. Additionally, when the state

variables are far from the desired path, TSMC provides a slower convergence time than SMC. To treat the singularity matter thoroughly, non-singular terminal sliding mode control (NTSMC) was established and successfully adopted in an effort to control nonlinear systems [28]–[30]. The remaining weak point was fast convergence time, which led to fast terminal sliding mode control (FTSMC) being applied to controlling uncertain, nonlinear second-order systems [31]–[33]. Unfortunately, the methods based on NTSMC and FTSMC only treat specific systems. Hence, to treat both singularity and fast convergence time simultaneously, the non-singular fast terminal sliding mode control (NFTSMC) system has been developed [34]–[38].

As a special consideration, undesired chattering occurred in practical systems whenever all the above control approaches (e.g., TSMC, FTSMC, NTSMC, NFTSMC) were applied with a large control gain in the corresponding reaching control law. A large amount of chattering can limit the robust behavior of the control system and attenuate performance significantly. For this reason, several capable algorithms such as the boundary layer technique [39]–[41], the high-order sliding mode [13], [41]–[43], and the disturbance observer [44] have been reported to cause a reduction in chattering. The weaknesses of the above-mentioned techniques sometimes present a challenging trade-off between chattering behavior attenuation and trajectory tracking accuracy, or else demanding an unrealistic magnitude of initial control input. However, there is an effective method to eliminate chattering behavior without the attenuation of the precision of the controlled system; the method applies an integral of a switching term to give chattering-free behavior such as Full-Order Sliding Mode (FOSM) [45].

It should be mentioned that all of the above-stated methods require prior knowledge of the bounded value of the uncertainties. To overcome this dependence, many kinds of SMC and TSMC methods using adaptive control have been introduced for the estimation of sliding gains [36], [40], [46]–[49] because of the estimated ability of the adaptive laws without the need for unrealistic assumptions.

Consequently, the motivation of our article is to propose a chattering-free, robust tracking control method that simultaneously eliminates the disadvantages of SMC and TSMC methods. In detail, a robust controller for uncertain nonlinear second-order systems must perform as follows:

- Removes the singularity weakness, provides fast convergence time, and states error with small oscillation along with robust behavior.
- Removes the dependency on essential knowledge of the upper bounded constants of unknown, uncertain terms.
- Gives chattering-free behavior without losing the robust behavior by adopting an integral of a switching term and an adaptive updating law.
- The convergence, the defined time stability, and the suggested adaptive adjustment law of the control system can be confirmed by the Lyapunov criterion.

The rest of our paper is presented as follows. The problem statements facilitated for the proposed PID-NFTSM function and the control law are presented in Section 2. Section 3 explains the design process of the suggested control method to obtain the desired output performance and to reject chattering behavior from the classic SMC. In Section 4, the suggested control method is applied to an uncertain nonlinear system [50]. Its simulated performance tracks a desired path to be compared to those methods based on the classical SMC [15], [18] and TSMC [26] methods to investigate positional errors, convergence time, rapid response, and chattering behavior reduction. Finally, Section 5 gives some conclusions of this paper.

II. PRELIMINARIES AND PROBLEM STATEMENT

This section presents some preliminary information and the problem statement, which is necessary for the controlling design.

Lemma 1 [51]: Suppose that a continuous positive-definite function $\Lambda(t)$ satisfies the following inequality:

$$\dot{Z}(t) \leq -\alpha Z^\gamma(t), \quad \forall t \geq t_0, Z(t_0) \geq 0, \quad (1)$$

in which $\alpha > 0, 0 < \gamma < 1$ are positive coefficients. Then for any given $t_0, Z(t)$ the following inequality is satisfied:

$$Z^{1-\gamma}(t) \leq Z^{1-\gamma}(t_0) - \alpha(1-\gamma)(t-t_0), \quad t_0 \leq t \leq t_1, \quad (2)$$

with $Z(t) = 0, \forall t \geq t_1$, and t_1 is computed by

$$t_1 = t_0 + \frac{1}{\alpha(1-\gamma)} Z^{1-\gamma}(t_0). \quad (3)$$

Lemma 2 ([52], Jensen's Inequality): The following expression holds:

$$\left(\sum_{i=1}^k \vartheta_i^{\beta_2} \right)^{1/\phi_2} \leq \left(\sum_{i=1}^k \vartheta_i^{\beta_1} \right)^{1/\phi_1}, \quad 0 < \phi_1 < \phi_2, \quad (4)$$

with $\vartheta_i \geq 0, 1 \leq i \leq k$.

Consider the following general nonlinear second-order system with disturbances and/or uncertainties ([45]):

$$\begin{cases} \dot{X}_1 = X_2 \\ \dot{X}_2 = \Pi(X, t) + \Phi(X, t) u^*(t) + \delta(X, t), \end{cases} \quad (5)$$

where $X = [X_1, X_2]^T \in R^n$ denotes the system state vector. $\Pi(X, t) \in R^n$ and $\Phi(X, t) \in R^{n \times n}$ are dynamic nonlinear smooth functions that have the corresponding expression as $\Pi(X, t) = \Pi_n(X, t) + \Delta\Pi(X, t)$ with $\Pi(0) = 0$, and $\Phi(X, t) u^*(t) = \Phi(X, t) u(t) + \Phi(X, t) \Delta u(t)$. The term $\Delta\Pi(X, t)$ indicates structural variation of the dynamic system, which is an uncertain term. The term of $\delta(X, t)$ indicates the disturbances and uncertainties, $u^*(t)$ is the actuation control input, $u(t)$ is the designed control value, and Δu is the input signal uncertainty.

In this paper, all anonymous terms are a function $L(X, \Delta u, \delta, t)$, which is termed as the lumped system uncertainty and defined as

$$L(X, \Delta u, \delta, t) = \Delta \Pi(X, t) + \Phi(X, t) \Delta u(t) + \delta(X, t). \quad (6)$$

From Eq. (6), the dynamics system of Eq. (5) can be represented as

$$\begin{cases} \dot{X}_1 = X_2 \\ \dot{X}_2 = \Pi_n(X, t) + \Phi(X, t) u(t) + L(X, \Delta u, \delta, t). \end{cases} \quad (7)$$

The central motivation of our article is that the proposed control system can provide high tracking precision for the system (7). Here, stated variables in (7) can approach the sliding function in a defined time. Then, those variables converge along the sliding function to the stable point regardless of disturbances and uncertainties.

The following constraint is assumed for the control approach design.

Assumption 1: There exists a known positive coefficient Γ_d such that the derivative of the $\Omega(X, \Delta u, \delta, t)$ function is bounded by

$$\left\| \frac{d}{dt} (\Omega(X, \Delta u, \delta, t)) \right\| \leq \Gamma_d, \quad (8)$$

where $\Omega(X, \Delta u, \delta, t)$ will be explained after Eq. (15).

III. DESIGN A CHATTERING-FREE, ADAPTIVE, ROBUST CONTROLLER USING THE PID-NFTSM FUNCTION

This section presents the approach to investigate the good features of both the PID and the NFTSM controllers as well as adaptive controllers. First, a new form of the sliding function is introduced. Second, a control method with an integral of a switching term and an adaptive updating law is designed to obtain the desired performance.

In this work, the PID sliding function is proposed as

$$\sigma = K_P s + K_I \int_0^t s d\phi + K_D \dot{s}, \quad (9)$$

where K_P , K_I , and K_D correspond to the proportional, integral, and derivative gain, respectively. $\sigma \in R^n$ is the PID-NFTSM sliding function, s is the first order NFTSM variable, and s is defined as [26]

$$s = X_2 + \kappa_1 X_1 + \kappa_2 (X_1)^{[\varphi]}, \quad (10)$$

with $0 < \varphi < 1$ a constant, $\kappa_1 = \text{diag}(\kappa_{11} \cdots \kappa_{1n}) \in R^{n \times n}$, $\kappa_2 = \text{diag}(\kappa_{21} \cdots \kappa_{2n}) \in R^{n \times n}$, $(X_1)^{[\varphi]} = \text{sign}(X_1)^\varphi$, and $\text{sign}(X_1)^\varphi$ is defined as [26]: $\text{sign}(X)^\varphi = [|X_1|^{\varphi_1} \text{sign}(X_1), \cdots, |X_n|^{\varphi_n} \text{sign}(X_n)]$, $i = 1, 2$.

The k^{th} element of the sliding surface of Eq. (10) is expressed as:

$$s_k = X_{2k} + \kappa_{1k} X_{1k} + \kappa_{2k} |X_{1k}|^{\varphi_k} \text{sign}(X_{1k}). \quad (11)$$

The first derivative of the first order NFTSM variable (10) is calculated as

$$\dot{s}_k = \dot{X}_{2k} + \kappa_{1k} X_{2k} + \kappa_{2k} X_{qk}, \quad (12)$$

where

$$X_{qk} = \begin{cases} \varphi_k |X_{1k}|^{\varphi_k-1} \dot{X}_{1k}, & \text{if } X_{1k} \neq 0 \\ 0, & \text{if } X_{1k} = 0. \end{cases} \quad (13)$$

Furthermore, Eq. (12) can be rewritten in the vector form as $\dot{s} = \dot{X}_2 + \kappa_1 X_2 + \kappa_2 X_q$.

The PID sliding function (9) is based on the NFTSM variables of Eq. (10), and thus it owns the values of both algorithms such as non-singularity, quick response, defined time convergence, robustness with uncertainties, and small steady-state error. These features are suitable and crucial for the controlling design because of its capability to compensate and quickly stabilize uncertain systems.

Substituting the derivative of the NFTSM variable (11) into (9) gives

$$\sigma = K_P s + K_I \int s + K_D (\dot{X}_2 + \kappa_1 X_2 + \kappa_2 X_q). \quad (14)$$

Substituting system (7) into (14) gives

$$\begin{aligned} \sigma &= K_P s + K_I \int s \\ &\quad + K_D \left(\begin{matrix} \Pi_n(X, t) + \Phi(X, t) u(t) \\ + L(X, \Delta u, \delta, t) + \kappa_1 X_2 + \kappa_2 X_q \end{matrix} \right) \\ &= K_P s + K_I \int s + K_D (\kappa_1 X_2 + \kappa_2 X_q) \\ &\quad + K_D (\Pi_n(X, t) + \Phi(X, t) u(t) + L(X, \Delta u, \delta, t)) \\ &= \Xi(X, s) + \Omega(X, \Delta u, \delta, t) \\ &\quad + K_D (\Pi_n(X, t) + \Phi(X, t) u(t)), \end{aligned} \quad (15)$$

where $\Xi(X, s) = K_P s + K_I \int s + K_D (\kappa_1 X_2 + \kappa_2 X_q)$, and $\Omega(X, \Delta u, \delta, t) = K_D L(X, \Delta u, \delta, t)$ indicates the anonymous terms in the system.

The following control law is developed for system (7) to achieve the desired performance:

$$u = -\Phi^*(X, t) (u_{eq} - K_D^{-1} u_{re}), \quad (16)$$

where $\Phi^*(X, t) = \Phi^T(X, t) [\Phi(X, t) \Phi^T(X, t)]^{-1}$ is pseudoinverse. The equivalent control law is constructed as

$$u_{eq} = K_D^{-1} \Xi(X, s) + \Pi_n(X, t), \quad (17)$$

and the continuous reaching control law is

$$\dot{u}_{re} + \Lambda u_{re} = \omega \quad (18)$$

and

$$\omega = -(\Gamma_d + \Gamma_T + \rho) \text{sign}(\sigma). \quad (19)$$

The initial value of $u_{re}(0)$ is chosen to be zero, Γ_d is a constant value which was stated as (8), and ρ is a small positive coefficient. $\Lambda \geq 0$ and Γ_T are chosen such that

$$\Gamma_T \geq \Lambda L_d. \quad (20)$$

Remark 1: From (18-19), u_{re} is obtained by adopting an integral of a switching term. Accordingly, the control system will achieve the chattering-free behavior.

Regarding the upper-bounded constants of both disturbances and uncertainties, an adaptive adjustment law is adopted to estimate those upper bounded values. Therefore, the system performance is always assured regardless of disturbances, uncertainties, and unknown terms influencing the control system.

A continuous adaptive reaching control law is designed as

$$\dot{u}_{re} + \Lambda u_{re} = \omega_a \tag{21}$$

and

$$\omega_a = -\left(\hat{\Gamma}_a + \rho\right) \text{sign}(\sigma), \tag{22}$$

in which $\hat{\Gamma}_a$ is the estimating value of the bounded constants $\Gamma_d + \Gamma_T$. $\hat{\Gamma}_a$ is adopted by the following updating law:

$$\dot{\hat{\Gamma}}_a = \frac{1}{\mu} |\sigma|, \tag{23}$$

where $\mu > 0$ indicates the adaptive gain.

Theorem 1: The uncertain nonlinear system (7) will quickly approach the sliding function in the defined time and then stabilize around zero within the defined time $\left(T \leq \frac{2V_2^{1/2}(0)}{\Upsilon}\right)$; if the satisfactory sliding function is proposed as (9), the control input signal is designed as (16-17, 21-22) with its corresponding adaptive adjustment law as (23), and there exist a bounded constant Γ^* satisfying the constraint (24).

$$\hat{\Gamma}_a \leq \Gamma^*. \tag{24}$$

This means that the robustness stability and the desired performance of the system (7) are always assured.

Proof: Adopting the control laws (16-17) and (21-22) to the sliding function (15) obtains

$$\begin{aligned} \sigma &= \Xi(X, s) + \Omega(X, \Delta u, \delta, t) \\ &+ K_D \left(\Pi_n(X, t) - \Phi(X, t) \Phi^*(X, t) \right. \\ &\quad \left. \times \left(K_D^{-1} \Xi(X, s) + \Pi_n(X, t) - K_D^{-1} u_{re} \right) \right) \\ &= u_{re} + \Omega(X, \Delta u, \delta, t). \end{aligned} \tag{25}$$

The result of Eq. (18) is presented by

$$\begin{aligned} u_{re}(t) &= \left(u_{re}(t_0) + (1/\Lambda) \left(\begin{matrix} \Gamma_d + \Gamma_T \\ + \rho \end{matrix} \right) \text{sign}(\sigma) \right) e^{t-t_0} \\ &\quad - (1/\Lambda) (\Gamma_d + \Gamma_T + \rho) \text{sign}(\sigma). \end{aligned} \tag{26}$$

Considering (20), (25-26) and the condition $u_{re}(0) = 0$, the following inequalities are achieved:

$$\Gamma_T \geq \Lambda L_d \geq \Lambda |u_{re}(t)|_{\max} \geq \Lambda |u_r(t)|. \tag{27}$$

With (21-22), the derivative of the sliding variable (25) gives

$$\dot{\sigma} = -\left(\hat{\Gamma}_a + \rho\right) \text{sign}(\sigma) - \Lambda u_{re} + \dot{\Omega}(X, \Delta u, \delta, t). \tag{28}$$

The estimated Error is described as

$$\tilde{\Gamma}_a = \hat{\Gamma}_a - (K_d + K_T). \tag{29}$$

The positive-definite Lyapunov functional is defined as

$$V_1 = \frac{1}{2} \sigma^T \sigma + \frac{\mu \tilde{\Gamma}_a^T \tilde{\Gamma}_a}{2}. \tag{30}$$

Utilizing the adaptive adjustment law (23), the derivative of sliding function (28), and the estimated error (29), the time derivative of the Lyapunov function (30) gives

$$\begin{aligned} \dot{V}_1 &= \sigma^T \dot{\sigma} + \mu \left(\hat{\Gamma}_a - (\Gamma_d + \Gamma_T) \right) \dot{\hat{\Gamma}}_a \\ &\quad \times \sigma^T \left(\begin{matrix} -\left(\hat{\Gamma}_a + \rho\right) \text{sign}(\sigma) \\ -\Lambda u_{re} + \dot{\Omega}(X, \Delta u, \delta, t) \end{matrix} \right) \\ &\quad + \left(\hat{\Gamma}_a - (\Gamma_d + \Gamma_T) \right) |\sigma| \\ &= (-\Lambda u_{re} \sigma - \Gamma_T |\sigma| - \rho |\sigma|) + \left(\begin{matrix} \dot{\Omega}(X, \Delta u, \delta, t) \sigma \\ -\Gamma_d |\sigma| \end{matrix} \right) \\ &\leq -\rho |\sigma|. \end{aligned} \tag{31}$$

The parameter ρ is assigned to be greater than zero, and thus, \dot{V}_1 will be negative. According to the Lyapunov principle, because \dot{V}_1 is negative σ and $\hat{\Gamma}_a$ will reach zero. This means that the estimated value of $\hat{\Gamma}_a$ has a bounded constant in Eq. (24). Next, it will be proved that system (7) will approach the sliding function within the defined time.

Consider the following Lyapunov function candidate as

$$V_2 = \frac{\sigma^T \sigma}{2} + \frac{\xi \tilde{\Gamma}_a^T \tilde{\Gamma}_a}{2}, \tag{32}$$

where ξ is a positive coefficient. With Eq. (24), the time derivative of Eq. (32) is derived similarly to obtain \dot{V}_1 as

$$\begin{aligned} \dot{V}_2 &= \sigma^T \dot{\sigma} + \mu \left(\hat{\Gamma}_a - \Gamma^* \right) \dot{\hat{\Gamma}}_a \\ &= \sigma^T \left(\begin{matrix} -\left(\hat{\Gamma}_a + \rho\right) \text{sign}(\sigma) \\ -\Lambda u_{re} + \dot{\Omega}(X, \Delta u, \delta, t) \end{matrix} \right) + \frac{\xi}{\mu} \left(\hat{\Gamma}_a - \Gamma^* \right) |\sigma| \\ &= (-\Lambda u_{re} \sigma - \Gamma_T |\sigma| - \rho |\sigma|) \\ &\quad + \left(\dot{\Omega}(X, \Delta u, \delta, t) \sigma - \Gamma_d |\sigma| \right) + \frac{\xi}{\mu} \left(\hat{\Gamma}_a - \Gamma^* \right) |\sigma| \\ &\leq -\rho |\sigma| + \frac{\xi}{\mu} \left(\hat{\Gamma}_a - \Gamma^* \right) |\sigma|. \end{aligned} \tag{33}$$

Because the estimated value $\hat{\Gamma}_a$ is bounded by Γ^* , (33) yields

$$\dot{V}_2 \leq -\rho |\sigma| + \frac{\xi}{\mu} \left(\hat{\Gamma}_a - \Gamma^* \right) |\sigma| \leq 0. \tag{34}$$

The parameters ρ, ξ are assigned to be greater than zero, so \dot{V}_2 will be negative:

$$\begin{aligned} \dot{V}_2 &\leq -\rho |\sigma| - \rho_1 \left| \hat{\Gamma}_a - \Gamma^* \right| \\ &\leq -\sqrt{2} \rho \frac{|\sigma|}{\sqrt{2}} - \rho_1 \sqrt{\frac{2}{\xi}} \sqrt{\xi} \frac{\left| \hat{\Gamma}_a - \Gamma^* \right|}{\sqrt{2}} \\ &\leq -\min \left\{ \sqrt{2} \rho, \rho_1 \sqrt{\frac{2}{\xi}} \right\} \cdot \left(\frac{|\sigma|}{\sqrt{2}} + \sqrt{\xi} \frac{\left| \hat{\Gamma}_a - \Gamma^* \right|}{\sqrt{2}} \right), \end{aligned} \tag{35}$$

where $\rho_1 = \frac{\xi}{\mu} |\sigma|$.

By using Jensen’s inequality in Lemma 2 and assigning $\Upsilon = \min \left\{ \sqrt{2}\rho, \rho_1 \sqrt{\frac{2}{\xi}} \right\}$, the following inequality can be achieved.

$$\begin{aligned} \dot{V}_2 &\leq -\Upsilon \left(\frac{\sigma^T \sigma}{(\sqrt{2})^2} + (\sqrt{\xi})^2 \frac{(\hat{\Gamma}_a - \Gamma^*)^T (\hat{\Gamma}_a - \Gamma^*)}{(\sqrt{2})^2} \right)^{\frac{1}{2}} \\ &\leq -\Upsilon V_2^{1/2}. \end{aligned} \tag{36}$$

Based on Lemma 1, it can be proved that the sliding variables in Eq. (9) will approach the PID-NFTSM function $\sigma = 0$ within the defined time $\left(T \leq \frac{2V_2^{1/2}(0)}{\Upsilon} \right)$. Additionally, when the PID-NFTSM function approaches zero, then the state variable system (10) will also stabilize around 0 in the defined time. This completes the proof of Theorem 1.

Remark 2: Once the PID-NFTSM function quickly approaches the stable point, the NFTSM variables will approach zero. For sliding variables defined by (10) ($s = X_2 + \kappa_1 X_1 + \kappa_2 (X_1)^{[\varphi]}$), X_1 is the system’s terminal attractor. The attaining time t_s that is taken to travel from $X_1(t_r) \neq 0$ to $X_1(t_r + t_s) = 0$ has been defined as [26]:

$$t_s = \frac{1}{\kappa_1(1-\varphi)} \ln \frac{\kappa_1 V^{1-\varphi}(X_0) + \kappa_2}{\kappa_2}, \tag{37}$$

where V is an extended Lyapunov description of the finite-time convergence, which can be given by $\dot{V}(X) + \kappa_1 V(X) + \kappa_2 V^\varphi(X) \leq 0, 0 < \varphi < 1$, with t_r defined as in [37].

Remark 3: In practical systems, the parameter drift matter has usually happened under the updating law (23). Therefore, the bounded method is performed to set up the updating law as

$$\dot{\hat{\Gamma}}_a = \begin{cases} 0 & \text{if } |\sigma| \leq \nu \\ \frac{1}{\mu} |\sigma| & \text{if } |\sigma| > \nu, \end{cases} \tag{38}$$

whereas $\nu > 0$ is an arbitrary positive value.

Remark 4: In this work, two control methodologies (PID-SMC and TSMC [26] shown in Appendix) used a boundary layer technique [39]–[41] to reject chattering behavior. This technique adopts a saturation function in the reaching control law instead of adopting a $sign(\sigma)$ function:

$$sat\left(\frac{\sigma}{\chi}\right) = \begin{cases} sign(\sigma) & \text{if } |\sigma| \geq \chi \\ \frac{\sigma}{\chi} & \text{if } |\sigma| < \chi, \end{cases} \tag{39}$$

in which χ is a minor positive coefficient. However, in some cases, the tracking error accuracy will be significantly reduced by using this technique. This technique will be analyzed in detail with numerical simulations.

IV. NUMERICAL SIMULATIONS

The suggested control algorithm can be applied to many systems, such as robotic manipulators, magnetic levitation systems, chaotic systems, etc. In the simulation section, some position tracking computer simulations for a three-link robot

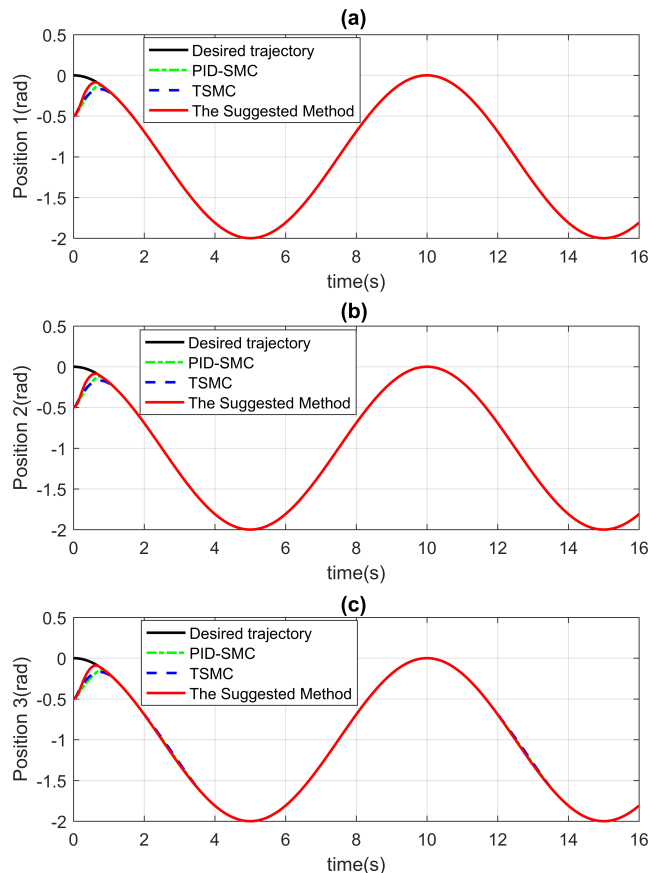


FIGURE 1. Tracking Positions in situation 1: (a) at Joint 1, (b) at Joint 2, and (c) at Joint 3.

manipulator have been performed to confirm the effectiveness of the proposed methodology.

For an n-link rigid robotic manipulator, the corresponding dynamic equation is given as ([16], [26])

$$M(\theta)\ddot{\theta} + C_m(\theta, \dot{\theta})\dot{\theta} + G(\theta) = \tau(t) + \tau_d(t), \tag{40}$$

where $\theta(t), \dot{\theta}(t), \ddot{\theta}(t) \in R^n$ denote the system’s state vectors. $M(\theta) = M_0(\theta) + \Delta M(\theta) \in R^{n \times n}$ is the positive definite inertia matrix and is symmetric, $C_m(\theta, \dot{\theta}) = C_0(\theta, \dot{\theta}) + \Delta C_m(\theta, \dot{\theta}) \in R^{n \times 1}$ indicates Coriolis and centrifugal forces, $G(\theta) = G_0(\theta) + \Delta G(\theta) \in R^{n \times 1}$ indicates gravitational force terms, $\tau(t) \in R^{n \times 1}$ indicates the control input torque, and $\tau_d(t) \in R^{n \times 1}$ indicates unknown disturbances. Here $M_0(\theta), C_0(\theta, \dot{\theta}), G_0(\theta)$ are nominal terms, whereas $\Delta M(\theta), \Delta C_m(\theta, \dot{\theta}), \Delta G(\theta)$ are dynamic uncertainties. Then, Eq. (40) can be represented as

$$\begin{aligned} M_0(\theta)\ddot{\theta} + C_0(\theta, \dot{\theta})\dot{\theta} + G_0(\theta) \\ = \tau(t) + \tau_d(t) + F(\theta, \dot{\theta}, \ddot{\theta}), \end{aligned} \tag{41}$$

whereas $F(\theta, \dot{\theta}, \ddot{\theta}) = \Delta M(\theta)\ddot{\theta} - \Delta C_m(\theta, \dot{\theta})\dot{\theta} - \Delta G(\theta) \in R^n$. Eq. (41) can be rewritten as

$$\begin{aligned} \ddot{\theta} = M^{-1}(\theta) [-C_0(\theta, \dot{\theta})\dot{\theta} - G_0(\theta)] \\ + M^{-1}(\theta)\tau(t) + M^{-1}(\theta)[\tau_d(t) + F(\theta, \dot{\theta}, \ddot{\theta})] \end{aligned} \tag{42}$$

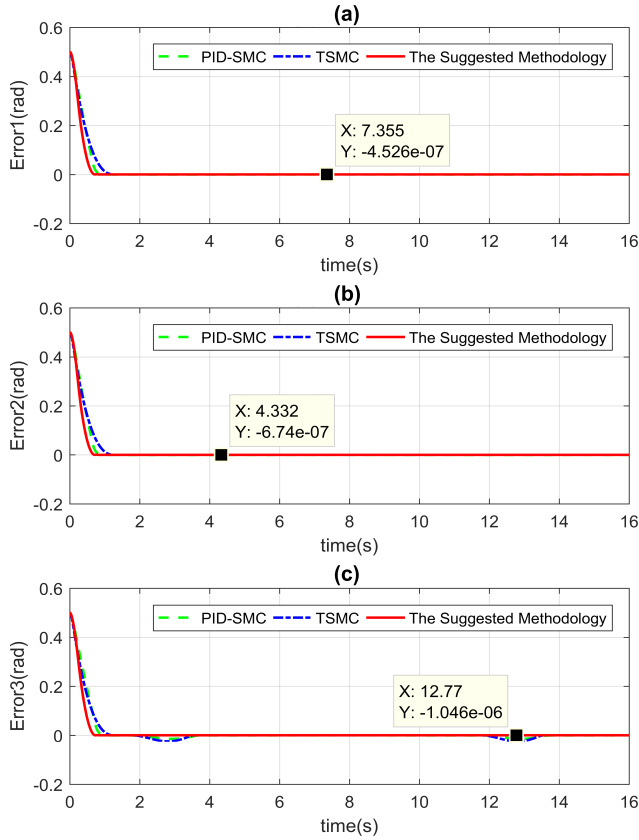


FIGURE 2. Tracking Errors in situation 1: (a) at Joint 1, (b) at Joint 2, and (c) at Joint 3.

To simplify the analysis and design in subsequent development, (42) can be expressed as

$$\ddot{\theta} = \Pi(\theta, \dot{\theta}) + \Phi(\theta)\tau(t) + \delta(\theta, \dot{\theta}, t), \quad (43)$$

where $\Pi(\theta, \dot{\theta}) = M^{-1}(\theta)[-C_0(\theta, \dot{\theta})\dot{\theta} - G_0(\theta)]$, $\Phi(\theta) = M^{-1}(\theta)$, and $\delta(\theta, \dot{\theta}, t) = M^{-1}(\theta)[\tau_d(t) + F(\theta, \dot{\theta}, \ddot{\theta})]$. $u^*(t) = \tau(t)$ is assigned to be the control input torque, and $X = [X_1, X_2]^T$ is the state variable vector with X_1, X_2 corresponding to $\theta, \dot{\theta} \in R^{n \times 1}$. Therefore, the robotic dynamic system (43) can be presented as

$$\begin{cases} \dot{X}_1 = X_2 \\ \dot{X}_2 = \Pi(X, t) + \Phi(X, t)u^*(t) + \delta(X, t), \end{cases} \quad (44)$$

where and $\Phi(X, t) \in R^{n \times n}$ are the smooth nonlinear vector fields and $\delta(X, t) \in R^n$ represents the disturbances and uncertainties.

It can be seen that (44) is exactly the same form of the general nonlinear second-order system (5). Consequently, the proposed control method can be directly applied to the robotic system (40).

In this work some position tracking computer simulations for a three-link robot manipulator were performed to show practicality and effectiveness of the suggested methodology. The dynamical model and crucial parameters of the robot was

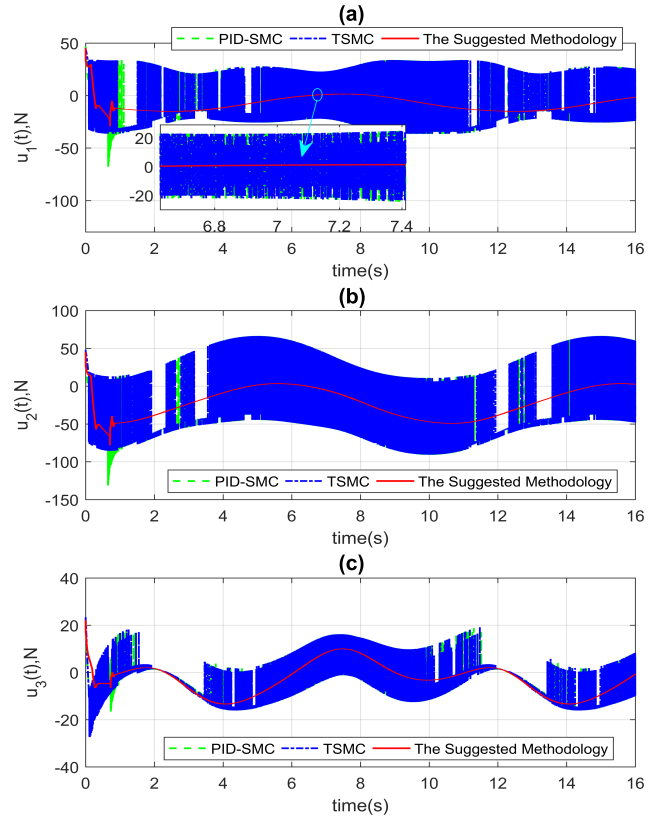


FIGURE 3. Control Input Signals in situation 1: (a) at Joint 1, (b) at Joint 2, and (c) at Joint 3.

reported previously [50]. All simulation studies were implemented in the MATLAB/Simulink software with a fixed-step size of 10^{-3} s. The Robot was only inspected when the first three joints and the last three joints were locked.

The reference joint paths for the position tracking are

$$\begin{cases} \theta_{d1} = \cos\left(\frac{t}{5\pi}\right) - 1 \\ \theta_{d2} = \sin\left(\frac{t}{5\pi} + \frac{\pi}{2}\right) - 1 \\ \theta_{d3} = \sin\left(\frac{t}{5\pi} + \frac{\pi}{2}\right) - 1. \end{cases} \quad (45)$$

Disturbances $\tau_d(t)$ and the dynamic uncertainties $F(\theta, \dot{\theta}, \ddot{\theta})$ at each joint are assumed to be

$$\begin{cases} \tau_{d1} + F_1 = 7.3 \sin(\dot{\theta}_1) + 7.5 \text{sign}(3\dot{\theta}_1) + 6.2\dot{\theta}_1 \\ \tau_{d2} + F_2 = 6.5 \sin(\dot{\theta}_2) + 8.3 \text{sign}(2\dot{\theta}_2) + 9.3\dot{\theta}_2 \\ \tau_{d3} + F_3 = 5.5 \sin(\dot{\theta}_3) + 3.5 \text{sign}(2\dot{\theta}_3) + 4.5\dot{\theta}_3. \end{cases} \quad (46)$$

The initial state variables of the robotic system were chosen as $\theta_1(0) = -0.5; \theta_2(0) = -0.5; \theta_3(0) = -0.5, \dot{\theta}_1(0) = \dot{\theta}_2(0) = \dot{\theta}_3(0) = 0$. The parameters of the PD-FTSM function (9-10) were experimentally chosen as $K_P = 15, K_I = 0.1, K_D = 0.5, \kappa_1 = 0.1, \kappa_2 = 2.2$ and $\varphi = 0.5$. The controlling input (16-17) and (21-22) are experimentally chosen with $\rho = 0.02, \Lambda = 0.5$ and other related parameters of the controller were chosen as same as

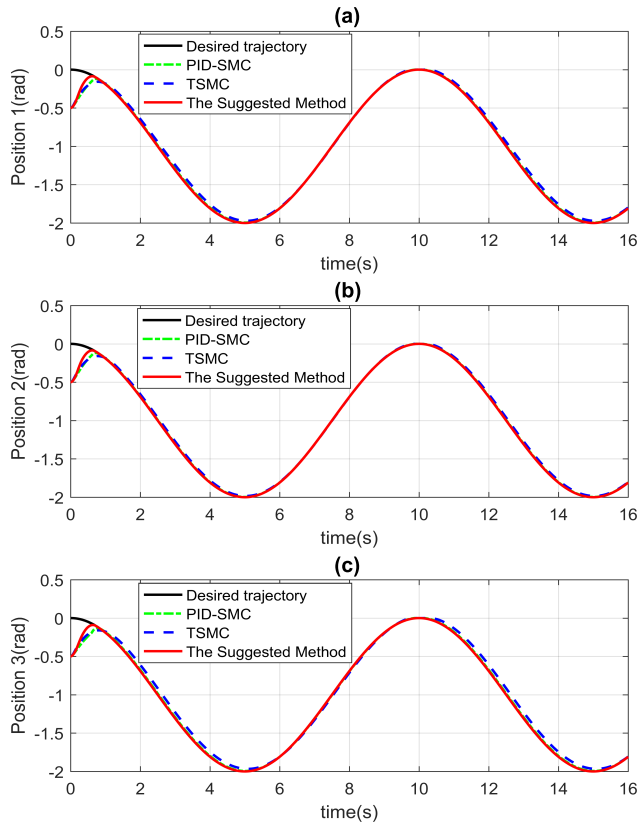


FIGURE 4. Tracking Positions in situation 2: (a) at Joint 1, (b) at Joint 2, and (c) at Joint 3.

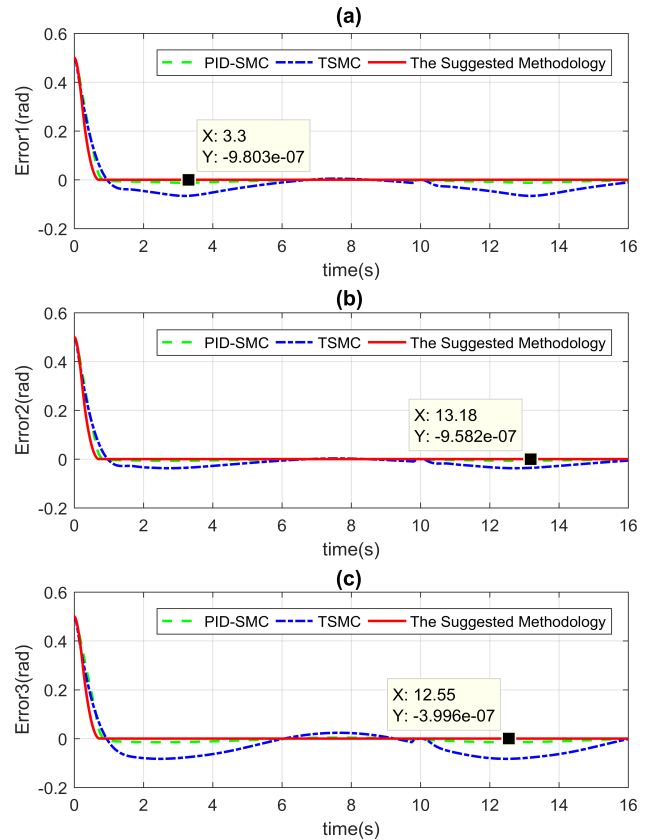


FIGURE 5. Tracking Errors in situation 2: (a) at Joint 1, (b) at Joint 2, and (c) at Joint 3.

the PID-FTSM function. The initial value of adaptive control law was chosen as $\hat{\Gamma}_a(0) = 0$, $\mu = 0.05$, and $\nu = 0.01$ to compensate and quickly stabilize uncertain systems.

To present the best capability of the proposed control algorithm, its reference trajectory performances were compared with PID-SMC that was based on the classical SMC [15], [18] and the TSMC [26] to inspect positional errors, convergence time, rapid response, and chattering-free behavior. These controllers for comparison have been briefly presented in Appendix.

The parameters of the sliding function and the PID-SMC were suitably selected from the simulated experiment as $K_P = 6.5$, $K_I = 0.01$, $K_D = 0.5$, $\Gamma = 10$, and $\rho = 0.02$ to similarly assign the initial control input magnitude and to achieve good simulation performance.

The parameters of the control method in [26] were suitably selected from the simulated experiment as $\beta = \text{diag}(0.5, 0.5, 0.5)$, $\gamma = 1.67$, $k_1 = \text{diag}(38, 65, 15)$, $\Gamma = 10$, and $\rho = 0.02$ to similarly assign the initial control input magnitude and to achieve good simulation performance.

The examples were simulated in two situations to analyze the effectiveness of the control methods in terms of both their chattering phenomenon and positional accuracies.

Situation 1: Each of three control methods has the $\text{sign}(\cdot)$ function in its reaching control term.

Situation 2: The proposed control methodology has the $\text{sign}(\cdot)$ function in its the reaching control law compared to both PID-SMC and TSMC [26] adopting Remark 4.

In Situation 1, the reference tracking positions and the corresponding tracking errors of the first three joints under all controllers are shown in Figs. 1-2. From Figures 1-2, it can be observed that all three control methods can reach and maintain the desired path. However, TSMC [26] and PID-SMC are less robust against large assumption uncertainties, while the suggested methodology has smaller position errors, (with $10^{-6} - 10^{-7}$ rad) compared to both mentioned controllers, by an order of $10^{-3} - 10^{-4}$ rad. Regarding chattering issues, a comparison of the control inputs in terms of the chattering phenomena is shown in Fig. 3. To obtain good simulation performance with the TSMC [26] and PID-SMC, the reaching control term required a large sliding gain that led to a significant chattering behavior. The chattering behavior from the suggested methodology was eliminated because this method applies a PID-FTSM function and an integral of a switching term.

The simulation results of Situation 2 verify the expected results illustrated in Figs. 4-6. In this Situation, the saturation function has been adopted in two control algorithms (PID-SMC and TSMC [26]) instead of the $\text{sign}(\cdot)$ function to reduce the chattering phenomena while the proposed

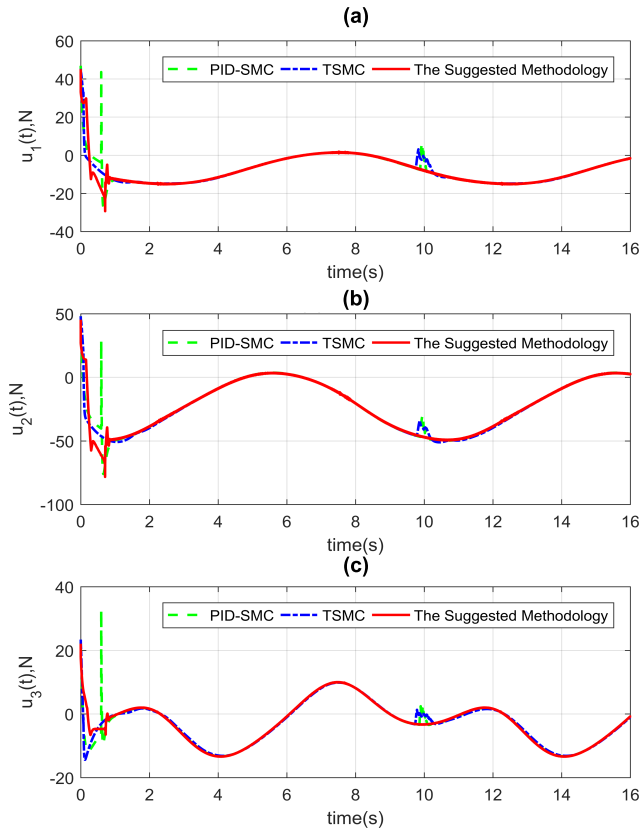


FIGURE 6. Control Input Signals in situation 2: (a) at Joint 1, (b) at Joint 2, and (c) at Joint 3.

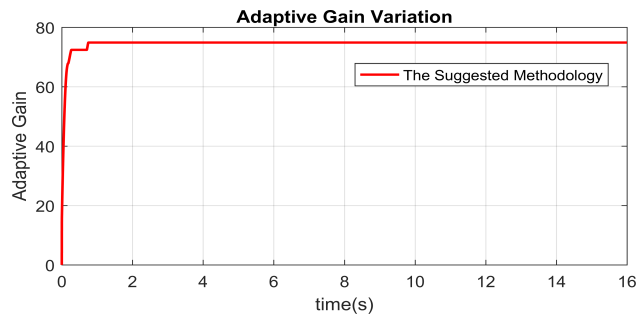


FIGURE 7. The response time of the estimating parameter.

methodology still adopts an integral of a switching term. However, as stated above, this technique decreases chattering behavior along with decreasing the robustness of the controllers. From Figs. 4-6, it is easy to anticipate that all three controllers will have a continuous control signal. It is noteworthy that the suggested control algorithm guarantees robustness with small steady-state errors, which are on the order of 10^{-6} rad, and chattering-free behavior, while those of the other controllers are worse, on the order of $10^{-2} - 10^{-3}$ rad.

Considering the bounded value of the uncertainties, the PID-SMC and TSMC control methods require prior knowledge of those bounded constants, but our suggested methodology does not. Therefore, the suggested

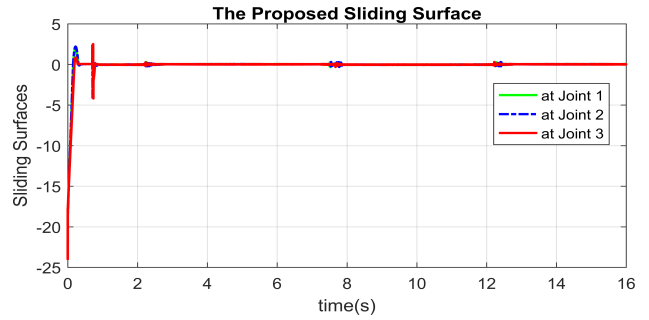


FIGURE 8. The response time of the proposed Sliding Surfaces: (a) at Joint 1, (b) at Joint 2, and (c) at Joint 3.

methodology will be more optimal than the other controllers. The variations of the approximated value are shown in Fig. 7. It can be observed that the values are approximated according to the variation of the unknown disturbances and uncertainties, and these approximated values will approach constant values along with the state variables reach to the PID-FTSM function.

The response time of the sliding surface is shown in Fig. 8.

From the simulation results, it is concluded that the suggested control methodology exhibits the best performance among the three control methods, including higher position precision, lower steady-state error, faster response, and chattering-free behavior.

V. CONCLUSION

This paper develops a chattering-free, adaptive, robust tracking control algorithm for a class of second-order nonlinear systems. In our algorithm, a novel sliding function, termed as a PID-Non-Singular fast terminal sliding (PID-NFTSM) function, is proposed to incorporate the good features of both the PID and the NFTSM approaches. Our proposed sliding function inherits some approaches in the field such as PID, NTSMC, and FTSMC to achieve non-singularity, fast response, defined time convergence, and stability with small steady-state error. To obtain a chattering-free behavior, a continuous method (with an integral of a switching term and adaptive updating law) have been applied to compensate for all of the anonymous uncertain components in the control system, such as disturbances, unmodeled dynamics, nonlinearities, and unmeasurable noise. Accordingly, the suggested method does not need prior information about the bound values of those anonymous components, along with chattering-free behavior, compared to other controllers. The experimental results for a PUMA560 robot manipulator confirm that the suggested methodology has more capability to adapt to many uncertain nonlinear systems with high accuracy.

APPENDIX
DESIGN PID-SMC

The PID based on SMC for the robotic manipulator (40) can be constructed as follows [15], [18].

Let $e(t) = \theta(t) - \theta_d(t)$ be the tracking positional error, with θ_d indicating the desired reference trajectory.

The following sliding function is considered as

$$s = K_P e + K_I \int_0^t e(t) dt + K_D \dot{e}, \quad (47)$$

in which K_P , K_I , and K_D are proportional gain, integral gain, and derivative gain matrices, respectively. The time derivative of Eq. (47) is computed as

$$\dot{s} = K_P \dot{e} + K_I e + K_D \ddot{e}. \quad (48)$$

To guarantee that the controlled variables of Eq. (47) converge to sliding variables, the following relations must be satisfied: $s = 0$ and $\dot{s} = 0$. The following proposed controller is based on the sliding mode design procedure

$$\tau(t) = \tau_{eq}(t) + \tau_{re}(t). \quad (49)$$

The term of the equivalent control of $\tau_{eq}(t)$ holds the trajectory of the error state variables on the sliding function, and it is computed with $\dot{s} = 0$ and $\delta(\theta, \dot{\theta}, t)$.

$$\dot{s} = K_P \dot{e} + K_I e + K_D \left(\frac{\Pi(\theta, \dot{\theta}) + \Phi(\theta) \tau(t)}{+\delta(\theta, \dot{\theta}, t) - \ddot{\theta}_d} \right) \quad (50)$$

Therefore, the term of the equivalent control of $\tau_{eq}(t)$ is designed as

$$\tau_{eq}(t) = -\Phi^{-1}(\theta) \left((\Pi(\theta, \dot{\theta}) - \ddot{\theta}_d) + \frac{K_I}{K_D} e + \frac{K_P}{K_D} \dot{e} \right), \quad (51)$$

and the reaching control term is designed as

$$\tau_{re}(t) = -\Phi^{-1}(\theta) (\Gamma + \rho) \text{sign}(s). \quad (52)$$

DESIGN TSMC AS FOLLOWS [26]

The control algorithm based on TSMC for the robotic manipulator (40) can be constructed as follows [24], [26]. Let $e(t) = \theta(t) - \theta_d(t)$ be the tracking positional error, with θ_d indicating the desired reference trajectory. The sliding function can be considered as

$$s = e + \beta \text{sig}(\dot{e})^\gamma, \quad (53)$$

where $\beta = \text{diag}(\beta_1, \beta_2, \dots, \beta_n)$ with $\beta_i > 0$, $1 < \gamma < 2$ and $\text{sig}(\dot{e})^\gamma = (|\dot{e}_1|^\gamma \text{sign}(\dot{e}_1), |\dot{e}_2|^\gamma \text{sign}(\dot{e}_2), \dots, |\dot{e}_n|^\gamma \text{sign}(\dot{e}_n))$.

The time derivative of Eq. (53) is computed as

$$\dot{s} = \dot{e} + \beta \gamma |\dot{e}|^{\gamma-1} \ddot{e}. \quad (54)$$

To guarantee that the controlled variables of Eq. (53) converge to sliding variables, the following relations must be satisfied: $s = 0$ and $\dot{s} = 0$.

The following proposed controller is based on the sliding mode design procedure

$$\tau(t) = \tau_{eq}(t) + \tau_{re}(t). \quad (55)$$

The term of the equivalent control of $\tau_{eq}(t)$ holds the trajectory of the error state variables on the sliding function, and it is computed with $\dot{s} = 0$ and $\delta(\theta, \dot{\theta}, t) = 0$.

$$\begin{aligned} \dot{s} &= \dot{e} + \beta \gamma |\dot{e}|^{\gamma-1} \ddot{e} \\ &= \dot{e} + \beta \gamma |\dot{e}|^{\gamma-1} (\Pi(\theta, \dot{\theta}) + \Phi(\theta) \tau(t) + \delta(\theta, \dot{\theta}, t) - \ddot{\theta}_d) \end{aligned} \quad (56)$$

Therefore, the term of the equivalent control of $\tau_{eq}(t)$ is designed as

$$\tau_{eq}(t) = -\Phi^{-1}(\theta) \left(\Pi(\theta, \dot{\theta}) - \ddot{\theta}_d + \frac{\beta^{-1}}{\gamma} |\dot{e}|^{2-\gamma} \right), \quad (57)$$

and the fast TSM reaching control term is designed as

$$\tau_{re}(t) = -\Phi^{-1}(\theta) (k_1 s + (\Gamma + \rho) \text{sign}(s)), \quad (58)$$

in which $k_1 = \text{diag}(k_{11}, k_{12}, k_{13})$, k_{1i} , Γ , and ρ are positive coefficients. Therefore, the TSM controller has the control input as

$$\tau(t) = -\Phi^{-1}(\theta) \left(\begin{aligned} &\Pi(\theta, \dot{\theta}) - \ddot{\theta}_d + \frac{\beta^{-1}}{\gamma} |\dot{e}|^{2-\gamma} \\ &+ k_1 s + (\Gamma + \rho) \text{sign}(s) \end{aligned} \right). \quad (59)$$

REFERENCES

- [1] Y. Su, P. C. Muller, and C. Zheng, "Global asymptotic saturated PID control for robot manipulators," *IEEE Trans. Control Syst. Technol.*, vol. 18, no. 6, pp. 1280–1288, Nov. 2010.
- [2] W. Yu and J. Rosen, "Neural PID control of robot manipulators with application to an upper limb exoskeleton," *IEEE Trans. Cybern.*, vol. 43, no. 2, pp. 673–684, Apr. 2013.
- [3] A. T. Vo, H.-J. Kang, and T. D. Le, "An adaptive fuzzy terminal sliding mode control methodology for uncertain nonlinear second-order systems," in *Proc. Int. Conf. Intell. Comput.*, Jul. 2018, pp. 123–135.
- [4] A. T. Vo, H.-J. Kang, and V.-C. Nguyen, "An output feedback tracking control based on neural sliding mode and high order sliding mode observer," in *Proc. 10th Int. Conf. Hum. Syst. Interact. (HSI)*, Jul. 2017, pp. 161–165.
- [5] T. D. Sanger, "Neural network learning control of robot manipulators using gradually increasing task difficulty," *IEEE Trans. Robot. Autom.*, vol. 10, no. 3, pp. 323–333, Jun. 1994.
- [6] K. Fujimoto and T. Sugie, "Iterative learning control of Hamiltonian systems: I/O based optimal control approach," *IEEE Trans. Autom. Control*, vol. 48, no. 10, pp. 1756–1761, Oct. 2003.
- [7] A. Tayebi, S. Abdul, M. B. Zaremba, and Y. Ye, "Robust iterative learning control design: Application to a robot manipulator," *IEEE/ASME Trans. Mechatronics*, vol. 13, no. 5, pp. 608–613, Oct. 2008.
- [8] M. Wang and A. Yang, "Dynamic learning from adaptive neural control of robot manipulators with prescribed performance," *IEEE Trans. Syst., Man, Cybern., Syst.*, vol. 47, no. 8, pp. 2244–2255, Aug. 2017.
- [9] F. Aghili, "Adaptive control of manipulators forming closed kinematic chain with inaccurate kinematic model," *IEEE/ASME Trans. Mechatronics*, vol. 18, no. 5, pp. 1544–1554, Oct. 2013.
- [10] L. A. Castañeda, A. Luviano-Juárez, and I. Chairez, "Robust trajectory tracking of a delta robot through adaptive active disturbance rejection control," *IEEE Trans. Control Syst. Technol.*, vol. 23, no. 4, pp. 1387–1398, Jul. 2015.
- [11] W. Shang, S. Cong, Y. Zhang, and Y. Liang, "Active joint synchronization control for a 2-DOF redundantly actuated parallel manipulator," *IEEE Trans. Control Syst. Technol.*, vol. 17, no. 2, pp. 416–423, Mar. 2009.
- [12] Y. Su, D. Sun, L. Ren, and J. K. Mills, "Integration of saturated PI synchronous control and PD feedback for control of parallel manipulators," *IEEE Trans. Robot.*, vol. 22, no. 1, pp. 202–207, Feb. 2006.
- [13] J. Li and Q. Zhang, "A linear switching function approach to sliding mode control and observation of descriptor systems," *Automatica*, vol. 95, pp. 112–121, Sep. 2018.
- [14] G. Sun, L. Wu, Z. Kuang, Z. Ma, and J. Liu, "Practical tracking control of linear motor via fractional-order sliding mode," *Automatica*, vol. 94, pp. 221–235, Aug. 2018.

- [15] C. Edwards and S. Spurgeon, *Sliding Mode Control: Theory and Applications*. Boca Raton, FL, USA: CRC Press, 1998.
- [16] S. Islam and X. P. Liu, "Robust sliding mode control for robot manipulators," *IEEE Trans. Ind. Electron.*, vol. 58, no. 6, pp. 2444–2453, Jun. 2011.
- [17] Y.-W. Liang, S.-D. Xu, D.-C. Liaw, and C.-C. Chen, "A study of T-S model-based SMC scheme with application to robot control," *IEEE Trans. Ind. Electron.*, vol. 55, no. 11, pp. 3964–3971, Nov. 2008.
- [18] V. I. Utkin, *Sliding Modes in Control and Optimization*. Berlin, Germany: Springer-Verlag, 2013.
- [19] A. Ferrara and G. P. Incremona, "Design of an integral suboptimal second-order sliding mode controller for the robust motion control of robot manipulators," *IEEE Trans. Control Syst. Technol.*, vol. 23, no. 6, pp. 2316–2325, Nov. 2015.
- [20] B. Xiao, Q. Hu, and Y. Zhang, "Adaptive sliding mode fault tolerant attitude tracking control for flexible spacecraft under actuator saturation," *IEEE Trans. Control Syst. Technol.*, vol. 20, no. 6, pp. 1605–1612, Nov. 2012.
- [21] B. B. Asik, M. A. Turan, H. Celik, and A. V. Katkat, "Effects of humic substances on plant growth and mineral nutrients uptake of wheat (*Triticum durum* cv. *Salihli*) under conditions of salinity," *Asian J. Crop Sci.*, vol. 1, no. 2, pp. 87–95, 2009. Accessed: Apr. 24, 2018. [Online]. Available: <http://scialert.net/qredirect.php?doi=ajcs.2009.87.95&linkid=pdf>
- [22] J. Li, Q. Zhang, X.-G. Yan, and S. K. Spurgeon, "Robust stabilization of T-S fuzzy stochastic descriptor systems via integral sliding modes," *IEEE Trans. Cybern.*, vol. 48, no. 9, pp. 2736–2749, Sep. 2018.
- [23] S. T. Venkataraman and S. Gulati, "Control of nonlinear systems using terminal sliding modes," *J. Dyn. Syst., Meas., Control*, vol. 115, no. 3, pp. 554–560, 1993.
- [24] M. Zhihong, A. P. Paplinski, and H. R. Wu, "A robust MIMO terminal sliding mode control scheme for rigid robotic manipulators," *IEEE Trans. Autom. Control*, vol. 39, no. 12, pp. 2464–2469, Dec. 1994.
- [25] Q. Xu, "Piezoelectric nanopositioning control using second-order discrete-time terminal sliding-mode strategy," *IEEE Trans. Ind. Electron.*, vol. 62, no. 12, pp. 7738–7748, Dec. 2015.
- [26] S. Yu, X. Yu, B. Shirinzadeh, and Z. Man, "Continuous finite-time control for robotic manipulators with terminal sliding mode," *Automatica*, vol. 41, no. 11, pp. 1957–1964, Nov. 2005.
- [27] H. Wang *et al.*, "Design and implementation of adaptive terminal sliding-mode control on a steer-by-wire equipped road vehicle," *IEEE Trans. Ind. Electron.*, vol. 63, no. 9, pp. 5774–5785, Sep. 2016.
- [28] Y. Feng, X. Yu, and Z. Man, "Non-singular terminal sliding mode control of rigid manipulators," *Automatica*, vol. 38, no. 12, pp. 2159–2167, Dec. 2002.
- [29] C.-K. Lin, "Nonsingular terminal sliding mode control of robot manipulators using fuzzy wavelet networks," *IEEE Trans. Fuzzy Syst.*, vol. 14, no. 6, pp. 849–859, Dec. 2006.
- [30] H. Wang, Z.-Z. Han, Q.-Y. Xie, and W. Zhang, "Finite-time chaos control via nonsingular terminal sliding mode control," *Commun. Nonlinear Sci. Numer. Simul.*, vol. 14, no. 6, pp. 2728–2733, 2009.
- [31] X. Yu and M. Zhihong, "Fast terminal sliding-mode control design for nonlinear dynamical systems," *IEEE Trans. Circuits Syst. I, Fundam. Theory Appl.*, vol. 49, no. 2, pp. 261–264, Feb. 2002.
- [32] S. Mobayen, "Fast terminal sliding mode controller design for nonlinear second-order systems with time-varying uncertainties," *Complexity*, vol. 21, no. 2, pp. 239–244, 2015.
- [33] T. Madani, B. Daachi, and K. Djouani, "Modular-controller-design-based fast terminal sliding mode for articulated exoskeleton systems," *IEEE Trans. Control Syst. Technol.*, vol. 25, no. 3, pp. 1133–1140, May 2017.
- [34] G. Sun, Z. Ma, and J. Yu, "Discrete-time fractional order terminal sliding mode tracking control for linear motor," *IEEE Trans. Ind. Electron.*, vol. 65, no. 4, pp. 3386–3394, Apr. 2018.
- [35] Z. He, C. Liu, Y. Zhan, H. Li, X. Huang, and Z. Zhang, "Nonsingular fast terminal sliding mode control with extended state observer and tracking differentiator for uncertain nonlinear systems," *Math. Problems Eng.*, vol. 2014, 2014, Art. no. 639707, doi: [10.1155/2014/639707](https://doi.org/10.1155/2014/639707).
- [36] B. Liang, Y. Zhu, Y. Li, P. He, and W. Li, "Adaptive nonsingular fast terminal sliding mode control for braking systems with electro-mechanical actuators based on radial basis function," *Energies*, vol. 10, no. 10, p. 1637, 2017.
- [37] L. Yang and J. Yang, "Nonsingular fast terminal sliding-mode control for nonlinear dynamical systems," *Int. J. Robust Nonlinear Control*, vol. 18, no. 16, pp. 557–569, 2010.
- [38] J. Zheng, H. Wang, Z. Man, J. Jin, and M. Fu, "Robust motion control of a linear motor positioner using fast nonsingular terminal sliding mode," *IEEE/ASME Trans. Mechatronics*, vol. 20, no. 4, pp. 1743–1752, Aug. 2015.
- [39] G. Edelbaher, K. Jezernik, and E. Urlep, "Low-speed sensorless control of induction machine," *IEEE Trans. Ind. Electron.*, vol. 53, no. 1, pp. 120–129, Feb. 2006.
- [40] H. Li, L. Dou, and Z. Su, "Adaptive nonsingular fast terminal sliding mode control for electromechanical actuator," *Int. J. Syst. Sci.*, vol. 44, no. 3, pp. 401–415, 2013.
- [41] V. Utkin, "Discussion aspects of high-order sliding mode control," *IEEE Trans. Autom. Control*, vol. 61, no. 3, pp. 829–833, Mar. 2016.
- [42] J. Davila, L. Fridman, and A. Levant, "Second-order sliding-mode observer for mechanical systems," *IEEE Trans. Autom. Control*, vol. 50, no. 11, pp. 1785–1789, Nov. 2005.
- [43] G. Rubio-Astorga, J. D. Sánchez-Torres, J. Cañedo, and A. G. Loukianov, "High-order sliding mode block control of single-phase induction motor," *IEEE Trans. Control Syst. Technol.*, vol. 22, no. 5, pp. 1828–1836, Sep. 2014.
- [44] J. Yang, S. Li, and X. Yu, "Sliding-mode control for systems with mismatched uncertainties via a disturbance observer," *IEEE Trans. Ind. Electron.*, vol. 60, no. 1, pp. 160–169, Jan. 2013.
- [45] Y. Feng, F. Han, and X. Yu, "Chattering free full-order sliding-mode control," *Automatica*, vol. 50, no. 4, pp. 1310–1314, Apr. 2014.
- [46] J. Zhang, Y. Lin, and G. Feng, "Analysis and synthesis of memory-based fuzzy sliding mode controllers," *IEEE Trans. Cybern.*, vol. 45, no. 12, pp. 2880–2889, Dec. 2015.
- [47] S. Mondal and C. Mahanta, "Adaptive second order terminal sliding mode controller for robotic manipulators," *J. Franklin Inst.*, vol. 351, no. 4, pp. 2356–2377, 2014.
- [48] S. Mobayen and F. Tchier, "A novel robust adaptive second-order sliding mode tracking control technique for uncertain dynamical systems with matched and unmatched disturbances," *Int. J. Control, Automat. Syst.*, vol. 15, no. 3, pp. 1097–1106, 2017.
- [49] R. Shahnazi, H. M. Shaneci, and N. Pariz, "Position control of induction and DC servomotors: A novel adaptive fuzzy PI sliding mode control," *IEEE Trans. Energy Convers.*, vol. 23, no. 1, pp. 138–147, Mar. 2008.
- [50] B. Armstrong, O. Khatib, and J. Burdick, "The explicit dynamic model and inertial parameters of the PUMA 560 arm," in *Proc. IEEE Int. Conf. Robot. Automat.*, vol. 3, Apr. 1986, pp. 510–518.
- [51] S. P. Bhat and D. S. Bernstein, "Finite-time stability of continuous autonomous systems," *SIAM J. Control Optim.*, vol. 38, no. 3, pp. 751–766, Jan. 2000.
- [52] E. M. Fels, "Beckenbach, E. F., and Bellman R.: Inequalities, Springer Verlag, Berlin-Göttingen-Heidelberg, 1961. (Hungarian Language Ignored) 276 Seiten, Preis 1 r. 9 k," *Biometrical J.*, vol. 8, no. 4, p. 279, 1966.



ANH TUAN VO received the B.S. degree in electrical engineering from the Danang University of Technology, Da Nang, Vietnam, in 2008. He is currently pursuing the Ph.D. degree with the School of Electrical Engineering, University of Ulsan, Ulsan, South Korea. His research interests include intelligent control, sliding mode control, robot fault diagnosis, and fault tolerant control.



HEE-JUN KANG received the B.S. degree in mechanical engineering from Seoul National University, South Korea, in 1985, and the M.S and Ph.D. degrees in mechanical engineering from The University of Texas at Austin, Austin, TX, USA, in 1988 and 1991, respectively. Since 1992, he has been a Professor of electrical engineering with the University of Ulsan. His current research interests are sensor-based robotic application, robot calibration, haptics, robot fault diagnosis, and mechanism analysis.

• • •